

# A New Inconsistency Measure for Linear Systems and Two Applications in Motion Analysis

Yan Niu

School of Computer Science  
University of Adelaide  
SA, Australia 5005

Email: yan.niu@adelaide.edu.au

Anthony Dick

School of Computer Science  
University of Adelaide  
SA, Australia 5005

Michael Brooks

School of Computer Science  
University of Adelaide  
SA, Australia 5005

**Abstract**—This paper proposes a new measure that continuously measures the degree of inconsistency for a linear system. We apply the new measure to two essential vision problems. One is to predict the fidelity of a local optical flow computation system; The other is to detect motion boundaries. Experimental results on benchmark sequences validate the performance of the proposed measure on both problems.

**Index Terms**—Optical flow, motion boundary, confidence measure, inconsistent linear system.

## I. INTRODUCTION

The linear system  $A\vec{X} = \vec{b}$  is a crucial model in a number of computer vision problems. With each equation of the system providing a constraint on the unknown vector  $\vec{X}$ , the problem is solved by finding the vector that best satisfies all the constraints. For example,  $\vec{X} = (A^T A)^{-1} A^T \vec{b}$  is one of the most widely used pseudo-solutions for  $A\vec{X} = \vec{b}$ .

However, in many cases, the system is ill-posed in the sense that:

- 1) The solution of the system is not unique. This happens when the system is deficient in independent constraints. Generally the deficiency can be detected by  $A$ 's rank-deficiency or infinite condition number. In real applications, due to the existence of noise, matrix  $A$  almost always has full rank. Thus rather than being rank deficient, it is more likely that the system is “well-posed but ill-conditioned”, where the condition number is large but finite.
- 2) The solution of the system does not exist. This happens when the system has “extra” constraints that are mutually contradictory. In this case, the pseudo-solution is severely distorted, as the system contains at least one constraint that is inconsistent with the true vector  $\vec{X}$ . It is thus important to detect the inconsistency before the pseudo-solution is applied. If inconsistency is detected, the linear system is not an appropriate model for the problem.

Mathematically, a necessary and sufficient condition for the system to be consistent is that the coefficient matrix  $A$  and the augmented matrix  $[A|\vec{b}]$  have the same rank. Thus it seems possible to detect inconsistency by counting the number of the non-trivial singular values of each matrix and taking the difference. However, unsatisfactory results are often obtained due

to the following factors. First, as pointed out by Shechtman-Irani in [1], the number of non-trivial eigenvalues depends on the predefined level of “being trivial”. A wrong threshold may lead to wrong rank detection. Second, rank comparison leads to a binary decision of consistency or inconsistency, which is inflexible. In real applications, due to the existence of noise, a small degree of inconsistency should be allowed; whereas if the system exhibits strong inconsistency beyond the noise level, it should be discarded.

In this paper, we use a different sufficient and necessary condition for  $A\vec{X} = \vec{b}$  to be consistent. Based on this, we derive a new COntstraint INconsistency (COIN) measure, which has the following advantages:

- Detects inconsistency due to solution non-existence;
- Provides a continuous measure of the *degree of inconsistency* of a system;
- Derivation is general—it works for any linear system;
- Does not require the linear system to be solved beforehand;
- Scale invariant;
- Low computational cost.

We discuss the application of the COIN measure (i) as a confidence measure for local optical flow computation; (ii) as a motion boundary detector. Experimental results on benchmark sequences validate the superior performance of the COIN measure to previous confidence measures and rank-increase measures on both problems.

## II. PROBLEM STATEMENT AND RELATED WORK

Let  $A\vec{X} = \vec{b}$  be a generic linear system, where  $A \in \mathbb{R}^{m \times n}$ ,  $\vec{b} \in \mathbb{R}^{m \times 1}$  are computed from the observed data, and  $\vec{X} \in \mathbb{R}^{n \times 1}$  is the unknown vector to be solved.

This linear system, although simple, is one of the most influential models in computer vision. A typical use of the linear system is for local optical flow computation, which assumes feature invariance (e.g., brightness [2], gradient [3]) over time and flow smoothness (e.g., constant [2], affine [4]) in a local neighbourhood. Under these assumptions, each pixel in the local patch provides a constraint for the velocity of the patch center, and the collection of the constraints forms a linear system. The accuracy of the solution that is obtained hinges on the well-posedness of the system. That is, the system should

have a solution that (i) exists; (ii) is unique; (iii) depends continuously on the observed data [5]. Thus to obtain an accurate estimate of the true vector  $\vec{X}$ , measures that evaluate the well-posedness of the system are needed.

Measuring the confidence that can be placed in a solution to a linear system has attracted significant attention in computer vision. However, this has focused mainly on inaccuracy caused by the non-uniqueness of the solution. In terms of optical flow, this corresponds to the notorious *aperture problem*. The fidelity of the pseudo-solution is generally measured by quantifying the rank deficiency of  $A$  [6]. For example, Lucas-Kanade use the least significant eigenvalue of  $A^T A$  [2]; Uras et al. use the condition number of  $A$  [3]; Bertero et al. and Barron et al. use the determinant [7] [8]; and Simioncelli use the trace [9]. All these measures aim at detecting the deficiency of independent constraints. If detected, one approach to obtain an unique solution is to integrate other constraints, such as regularized variation of the flow field, with the system [7].

Except for the condition number measure, these methods neglect the ambiguity caused by the system's scale. More specifically, systems  $A\vec{X} = \vec{b}$  and  $\alpha A\vec{X} = \alpha\vec{b}$  ( $\alpha \neq 0$ ) have same solution manifolds and are always solved by the same pseudo-solution. Hence the confidence measure of a solution should be independent of the scaling factor  $\alpha$ . However, the smallest eigenvalue measure, the trace measure and the determinant measure are all affected by  $\alpha$ , which consequently leads to ambiguity.

Moreover, measuring confidence by solution uniqueness implicitly assumes that the system has solution(s). Unfortunately, this is quite often not true. In the context of optical flow, if a local patch contains motion boundaries, the system is prone to collect constraints that are valid for some neighbouring pixels but invalid for the center pixel, as they are from different motion segments. Research in this area has focused on finding a solution that better tolerates the invalid constraints (e.g., [10]). Such a methodology, although it may find a solution that is less inaccurate, is *unable to obtain an accurate solution from an invalid system*. A more practical approach is to predict the inconsistency, and replace the invalid system by a more appropriate model. However, to our best knowledge, the only attempt to measure the system inconsistency is Haussecker et al.'s *coherency measure* and *corner measure* [11], which are specific to 3D structure tensors. In contrast to previous work, the proposed COIN measure is based on a general theory on the consistency of a linear system, and hence can be applied to any local optical flow computation technique formulated in this way.

Research has also been carried out on measuring the certainty of a flow vector *after* flow computation. In [12] and [13], such measures are defined as the inverse of specially designed energy terms associated with particular optical flow techniques. In [14], [15], the fidelity of a computed flow vector is measured by its conformity to neighbouring flow vectors, according to a linear subspace or a statistical model. These measures, although they can be applied to the flow obtained by any method, require training data to learn the parameters

of the models. Moreover, they can only be applied to dense flow field computation. In contrast, the COIN measure predicts the reliability of a flow vector before it is recovered, which is important for the algorithm to discard inappropriate constraints before flow computation. Furthermore, it does not require dense precomputation of flow vectors in the neighborhood.

We also apply the proposed measure as a simple motion boundary detection method. A related line of work is Shechtman-Irani's rank-increase measure [1], which measures motion inconsistency in the framework of human behavior recognition:

$$\Delta r = \frac{\det(T_{3D})}{\det(T_{2D})\lambda_l},$$

where  $T_{2D}$  and  $T_{3D}$  denote the Lucas-Kanade 2D and 3D structure tensor [2], and  $\lambda_l$  is the largest eigenvalue of  $T_{3D}$ . The proposed measure and the rank-increase measure are related in the sense that, if the linear system  $A\vec{X} = \vec{b}$  degenerates to Lucas-Kanade's optical flow computation [2], both measures detect motion inconsistency by comparing the continuous rank difference between the 2D structure tensor and 3D structure tensor. However, the two measures are fundamentally different in the following aspects. First, the proposed measure is not limited to Lucas-Kanade's system. The arrays  $A$  and  $\vec{b}$  can be generated by the model that best suits the underlying data, e.g., piecewise affine or planar motion model; whereas the rank-increase measure is limited to 2D and 3D structure tensor. Second, the two measures have different definitions rooted from different mathematical theories. The rank-increase measure is based on the *interlacing property* of symmetric matrices (pp.396, [16]), and the definition does not take "divided by zero" into consideration; whereas the proposed measure is based on the projection of  $\vec{b}$  to the column space of  $A$ , and avoids zeros in the denominator. Third, the rank increase measure works well if the camera motion is negligible relative to the object motion, but results in false positive detection if the camera undergoes fast motion and the background lacks spatial texture. In this case, both  $\lambda_l$  and  $\frac{\det(T_{3D})}{\det(T_{2D})}$  correspond to the temporal eigenvalue [17]. As a consequence, the measure value is near to 1, which indicates motion inconsistency even if the background undergoes uniform motion. On the contrary, the proposed measure is robust to fast camera motion.

### III. A NEW CONSTRAINT INCONSISTENCY MEASURE

In theory, a necessary and sufficient condition for the linear system  $A\vec{X} = \vec{b}$  to be consistent is that the coefficient matrix  $A$  and the augmented matrix  $[A|\vec{b}]$  have the same rank (see p.277, [18] for proof). However, in real applications, due to the existence of noise,  $A$  and  $[A|\vec{b}]$  are always of full rank. Furthermore, if  $m > n$ , both matrices have rank equal to the number of their columns. Hence there is always rank increase from  $A$  to  $[A|\vec{b}]$ . A practical approach is to map inconsistency to a continuous measure, which can be used to judge whether the inconsistency comes from noise or contradicted constraints. Aiming at such a measure, we

propose another necessary and sufficient condition for the system to be consistent.

*Theorem 1:* Define  $\vec{p} = A^T \vec{b}$ ,  $G = A^T A$ , and let real numbers  $\lambda_1 \geq \dots \geq \lambda_n$  be the sorted eigenvalues of  $G$  and  $\vec{e}_1, \dots, \vec{e}_n$  be the corresponding orthonormal eigenvectors. Define  $\theta$  by

$$\theta = \sum_{i=1}^r \frac{(\vec{p}^T \cdot \vec{e}_i)^2}{\lambda_i}, \text{ where } r = \text{rank}(A). \quad (1)$$

System  $A\vec{x} = \vec{b}$  is consistent if and only if  $\|\vec{b}\|_2^2 = \theta$ .

*Proof:* Let  $A = USV^T$  be the singular value decomposition of  $A$ , where  $U$  and  $V$  are orthogonal matrices and the diagonal matrix  $S$  contains the non-zero singular values of  $A$ , i.e.,  $\sqrt{\lambda_1}, \sqrt{\lambda_2}, \dots, \sqrt{\lambda_r}$ .

Denote the  $i$ th column of  $U$  by  $\vec{u}_i$ .  $\text{rank}(A) = \text{rank}([A|\vec{b}])$  if and only if  $\vec{b}$  is in the column space of  $A$ , which is spanned by the first  $r$  columns of  $U$ . That is,

$$\begin{aligned} \text{rank}(A) &= \text{rank}([A|\vec{b}]) \\ &\Updownarrow \\ \|\vec{b}\|_2^2 &= \sum_{i=1}^r (\vec{b}^T \vec{u}_i)^2; \end{aligned} \quad (2)$$

Note that  $G = A^T A = VS^2V^T$ , and hence matrix  $V$  contains the eigenvectors of  $G$ , i.e.,

$$V = [\vec{e}_1 \quad \vec{e}_2 \quad \dots \quad \vec{e}_n]. \quad (3)$$

It can then be easily verified that

$$A\vec{e}_i = USV^T \vec{e}_i = \sqrt{\lambda_i} \vec{u}_i. \quad (4)$$

By the definition of  $\vec{p}$ , Eq.4 leads to

$$\vec{p}^T \vec{e}_i = \vec{b}^T A\vec{e}_i = \sqrt{\lambda_i} \vec{b}^T \vec{u}_i. \quad (5)$$

Recall Eq. 2, thus

$$\sum_{i=1}^r \frac{(\vec{p}^T \vec{e}_i)^2}{\lambda_i} = \sum_{i=1}^r (\vec{b}^T \vec{u}_i)^2 = \|\vec{b}\|_2^2 \Leftrightarrow \text{rank}(A) = \text{rank}([A|\vec{b}]) \quad (6)$$

Eq.6 proves that

$$\text{rank}(A) = \text{rank}([A|\vec{b}]) \Leftrightarrow \|\vec{b}\|_2^2 = \theta.$$

This proves Theorem 1. ■

The theorem has a direct corollary as stated below.

*Corollary 2:* For any vector  $\vec{b}$  and  $\theta$  defined as in Theorem 1,  $\|\vec{b}\|_2^2 \geq \theta$ .

*Proof:* With the same notations as in the proof of Theorem 1, the columns of  $U$  form an orthogonal basis of  $\mathbb{R}^{m \times m}$ . Hence any vector  $\vec{b} \in \mathbb{R}^{m \times 1}$  satisfies

$$\|\vec{b}\|_2^2 = \sum_{i=1}^m (\vec{b}^T \vec{u}_i)^2 \geq \sum_{i=1}^r (\vec{b}^T \vec{u}_i)^2. \quad (7)$$

Substituting Eq.6 into the R.H.S. of the inequality, the following inequality can be easily verified.

$$\|\vec{b}\|_2^2 \geq \theta. \quad (8)$$

Theorem 1 states that  $\|\vec{b}\|_2^2$  can not take any arbitrary value if the system is expected to have solution(s). In other words, for the system to be solvable,  $\|\vec{b}\|_2^2$  must equal an ideal value  $\theta$ . Theoretically, if the constraints in  $A\vec{X} = \vec{b}$  are strictly consistent, then  $\|\vec{b}\|_2^2 - \theta$  is exactly zero, and vice versa. However, due to the existence of noise, each constraint is a noisy observation of the true underlying data. Therefore, it is more practical to allow  $\|\vec{b}\|_2^2 - \theta = n_\epsilon$ , where  $n_\epsilon$  is a noise signal of small magnitude. Otherwise, large magnitude of  $\|\vec{b}\|_2^2 - \theta$  is evidence for rank increase from the coefficient matrix to the augmented matrix, and hence the inconsistency of the constraints can be inferred. Therefore our COIN (Constraint INconsistency) measure is defined by

$$m = \|\vec{b}\|_2^2 - \theta. \quad (9)$$

It can be shown that the COIN measure depends continuously on the underlying data, which is important to indicate the degree of inconsistency of a linear system faithfully. It also has the advantage of low computational cost, as it uses the eigendecomposition  $A^T A$  only; whereas the rank comparison of  $A$  and  $[A|\vec{b}]$  requires the SVD of both matrices.

It is worth noting that  $\theta$ , which is the projection of  $\vec{b}$  to the column space of  $A$ , coincides with the least squares solution of the system  $Ax = b$ . In practice, it can therefore also be obtained as  $AA^+ \vec{b}$ , where  $A^+$  is the Penrose-Moore pseudoinverse, or by other methods for calculating a least squares solution and residual.

#### IV. TWO APPLICATIONS OF THE COIN MEASURE

In this section, we discuss the applications of the COIN measure to two fundamental motion problems: (1) local optical flow computation confidence measure, (2) motion boundary detection. First, we illustrate the formulation of a local optical flow system by Lucas-Kanade's pioneering work.

##### A. The COIN measure for LK system

The basic optical flow constraint states that each pixel corresponding to a fixed location on a moving surface has constant brightness over time. Denoting image intensity at spatial-temporal position  $(x, y, t)$  by  $E(x, y, t)$ , this can be written as:

$$\frac{dE}{dt} = E_x x_t + E_y y_t + E_t = 0, \quad (10)$$

where the subscripts denote the corresponding partial derivatives, and  $(x_t, y_t)$  is the pixel's flow vector to be solved. Additionally, Lucas-Kanade assume that the flow is locally constant. Thus each neighbouring pixel in the local area contributes another constraint on  $(x_t, y_t)$ . The collection of all the constraints form a linear system  $A\vec{X} = \vec{b}$ , where

$X = (x_t, y_t)$ . In this linear system,  $A^T A$  and  $[A|\vec{b}]^T [A|\vec{b}]$  are 2D and 3D structure tensors, i.e.,

$$\begin{aligned} A^T A &= \begin{bmatrix} \sum E_x E_x & \sum E_x E_y \\ \sum E_x E_y & \sum E_y E_y \end{bmatrix}; \\ [A|\vec{b}]^T [A|\vec{b}] &= \begin{bmatrix} \sum E_x E_x & \sum E_x E_y & \sum E_x E_t \\ \sum E_x E_y & \sum E_y E_y & \sum E_y E_t \\ \sum E_x E_t & \sum E_y E_t & \sum E_t E_t \end{bmatrix} \end{aligned} \quad (11)$$

where the summation is taken over the local area. Let  $\lambda_1 \geq \lambda_2$  be the eigenvalues of the 2D structure tensor, and  $\vec{e}_1, \vec{e}_2$  be the corresponding eigenvectors. The COIN measure in this example is given by

$$m = \begin{cases} \sum E_t^2 & \text{if } \text{rank}(A) = 0; \\ \sum E_t^2 - \sum_{i=1}^r \frac{(\vec{p} \cdot \vec{e}_i)^2}{\lambda_i} & \text{if } \text{rank}(A) = r; \end{cases} \quad (12)$$

where  $\vec{p} = [\sum E_x E_t \quad \sum E_y E_t]$ .

If we apply Theorem 1 to this example, the following Corollary seems straightforward, by noting that  $\text{rank}(A^T A) = \text{rank}(A)$  and  $\text{rank}([A|\vec{b}]^T [A|\vec{b}]) = \text{rank}([A|\vec{b}])$ .

*Corollary 3:* The Lucas-Kanade system is consistent if and only if the 2D and 3D structure tensors have same rank.

Since the advent of Lucas-Kanade flow computation, many sophisticated local flow models have been proposed. Commonly, they are modeled as solving a linear system  $A\vec{X} = \vec{b}$ , where  $A$  and  $\vec{b}$  contain the spatial and temporal derivatives of  $E$  at several positions, and  $\vec{X}$  is the unknown vector of motion parameters. The connection between the motion inconsistency and constraint inconsistency, thus can be generalized to these local optical flow systems.

### B. Confidence Measure for Local Optical Flow Computation

If a linear system  $A\vec{X} = \vec{b}$  is inconsistent, the estimated solution will not be accurate. In general, the more inconsistent the system, the more distorted the solution. Based on this observation, we measure the confidence of the recovered flow by the system's consistency.

As discussed in Section II, a proper confidence measure should be free of the scaling ambiguity. Therefore, we normalize  $\vec{b}$  to unit norm and scale  $A$  accordingly, if  $\|\vec{b}\|_2 \neq 0$ .

If  $\|\vec{b}\|_2 = 0$ ,  $A$  and  $[A|\vec{b}]$  must have the same rank, and so our confidence measure is defined by

$$c = \begin{cases} 1, & \text{if } \|\vec{b}\|_2 = 0. \\ 1 - \frac{m}{\|\vec{b}\|_2^2}, & \text{otherwise.} \end{cases} \quad (13)$$

where  $m$  is the COIN measure. By Corollary 2, it can be verified that  $c \in [0, 1]$ , where a small  $c \rightarrow 0$  indicates the low confidence of the computed flow.

### C. Motion Boundary Detection

For long, it has been noticed that if the 3D structure tensor has full rank, then the local spatial-temporal patch has *no* coherent motion (e.g., [11]). In [1], Shechtman and Irani generalized this observation by pointing out that, if the 3D

structure tensor has higher rank than the 2D structure tensor, then there is no coherent motion in the patch. The rationale of the generalization, however, is based on a case by case study of all possible ranks that the structure tensors can have (Section 4, [1]). Section IV-A sheds a different light on Shechtman and Irani's theory. That is, the 3D structure tensor's rank increase, which implies lack of coherent motion, is just another expression of the inconsistency among the optical flow constraints in Lucas-Kanade's system.

Therefore, the COIN measure can be applied to the same problem as a generalization of the rank-increase measure. In [1], the motion inconsistency is defined in the framework of human behavior similarity, whereas in this work we apply the COIN measure to motion boundary detection, with the large COIN value signaling a high probability of a motion boundary's presence. Unlike the confidence measure, the motion inconsistency score is not normalized by  $\|\vec{b}\|_2^2$ , due to the fact that  $\alpha A\vec{X} = \alpha\vec{b}$  ( $\alpha \neq 0$ ) exhibits different degree of inconsistency when  $\alpha$  varies.

## V. EXPERIMENTAL RESULTS

### A. Measuring Flow Confidence

We compare the normalized COIN measure to other classical confidence measures on benchmark sequences: RubberWhale, Hydrangea, Grove2, Grove3 [19], Street [20] and Yosemite [21]. The measures are least significant eigenvalue [2], determinant [8], inverse condition number [3] and the corner measure [11], with large value indexing high confidence.

To have a fair comparison with the corner measure, which is specific to the 3D structure tensor, we employ Lucas-Kanade's flow technique to recover the flow field. To evaluate the performance quantitatively, we follow the routine of "sparsification" used in [1] and [15]. That is, given the confidence scores over the whole image, we remove the  $n\%$  ( $n = 0, \dots, 99$ ) pixels that have the lowest scores, and compute the average flow error of the remaining pixels.<sup>1</sup> The end-point error  $e$  at a pixel  $(i, j)$  is given by the Euclidean distance between the true flow  $\vec{t}(i, j)$  and the computed flow  $\vec{c}(i, j)$ , i.e.,

$$e(i, j) = \|\vec{t}(i, j) - \vec{c}(i, j)\|_2.$$

If the scoring scheme works well, the removal is expected to decrease the average error of the remaining flow vectors. In the ideal case, pixels that have the smallest confidence scores are exactly the pixels that have the largest errors. This ideal case provides an optimal score  $C_{opt}(i, j) = 1 - e(i, j) / \max_{(i, j)}(e(i, j))$  as a benchmark [15].

As some measures (the least significant eigenvalue, determinant and inverse condition number) depend on the ill-condition of the system (the aperture problem), whereas others (the corner measure and the normalized COIN) depend on the inconsistency of the system (the motion boundary problem), it seems that different choices of the local patch size may favor

<sup>1</sup>On RubberWhale and Hydrangea, some pixels' ground truth flows are unknown, which are coded as the black color. These pixels are excluded from our error statistics.

different measures – a small patch is more likely to suffer the aperture problem than the motion boundary problem, whereas a large patch is in the opposite situation. To test that, we conducted experiments by varying the patch size from  $7 \times 7$  to  $19 \times 19$  gradually. Our experiments show that on all sequences except RubberWhale, the ranking of different measures is not affected by the patch size selection. On RubberWhale sequence, the comparison between the corner measure and the normalized COIN measure is slightly affected by the size of the patch, when  $n > 70\%$ . Fig. 1 plots the average errors during the sparsification course on RubberWhale, Hydrangea and Yosemite, where flow is computed on  $7 \times 7$  and  $19 \times 19$  patches.

Fig. 2 presents the results on Sequences Grove2, Grove3 and Street, where the local patch size for flow computation is  $7 \times 7$ . On these sequences, as well as Hydrangea, the normalized COIN measure outperforms the other measures uniformly. Experiments are also conducted on Urban2 and Urban3 [19]. However, as the motion of these two sequences are too large to be recovered by LK with reasonable accuracy, the confidence measure on the computed flow does not make much sense.

### B. Motion Boundary Detection

To quantitatively evaluate the performance of the COIN measure on motion boundary detection, we need to compare the detected motion boundary to the ground truth. Different from manually labeling the frames, we generate the ground truth from the optical flow of benchmark sequences. Specifically, at each pixel  $(i, j)$ , we compute the spatial variation of the ground truth flow  $(u(i, j), v(i, j))$  by

$$\Delta(i, j) = |u_x(i, j)| + |u_y(i, j)| + |v_x(i, j)| + |v_y(i, j)|, \quad (14)$$

and threshold  $\Delta(i, j)$  over the whole image, with the partial derivatives in Eq. 14 approximated by central differencing (forward or backward differencing at image boundaries). Fig 3 shows the ground truth flow and the motion boundary obtained from widely used benchmark sequences.

We compare the COIN measure to the rank-increase measure. Particularly, at each pixel, the 2D and 3D structure tensors are computed from the intensity. The COIN measure (Eq. 12) and the rank-increase measure are calculated from the tensors' eigen-systems. As large values of both measures indicating high level of motion inconsistency, we vary the thresholds for both measures, and label the pixels that pass the thresholding as detected motion boundary pixels. The recall-precision rates are computed for both detection scores, as demonstrated in Fig 3. Experiments are conducted on RubberWhale, Hydrangea, Grove2, Grove3, Urban2, Urban3 and Street. On all sequences except Street, the COIN measure achieves superior performance. Note that on sequence Hydrangea, the rank increase measure's detection is rather unsatisfactory. The reason is as analyzed in Section II. The background in the sequence is under a camera motion at about 4 pixels/frame, but is lack of texture compared to the other moving object, the Hydrangea. This problem is avoided on

sequence street, as the background's velocity ( $\approx 1$  pixel/frame) is slower than the foreground ( $\approx 2$  pixels/frame), but has richer spatial textures. Unlike the rank-increase measure, the COIN measure performs stably even when the camera undergoes fast motion.

## VI. CONCLUSION

This paper has derived a novel measure for inconsistency in linear systems of equations, and shown that when applied to Lucas-Kanade flow computation, it can be used to predict the confidence with which flow can be recovered at each point in an image. Analysis suggests and experimental results confirm that it outperforms other measures that have been previously used for this task, and that it can also be used as a simple and effective motion boundary detector. In future we plan to experiment with other linear systems that occur in computer vision problems.

## REFERENCES

- [1] E. Shechtman and M. Irani, "Space-time behavior based correlation or how to tell if two underlying motion fields are similar without computing them?" *IEEE Trans. on Pattern Analysis and Machine Intelligence*, vol. 29, pp. 2045–2056, Nov. 2007.
- [2] B. Lucas and T. Kanade, "An iterative image registration technique with an application to stereo vision," in *DARPA Image Understanding Workshop*, 1981, pp. 121–130.
- [3] S. Uras, F. Girosi, A. Verri, and V. Torre, "A computational approach to motion perception," *Biol. Cybern.*, pp. 79–87, 1988.
- [4] M. Campani and A. Verri, "Computing optical flow from an overconstrained system of linear algebraic equations," in *Intl. Conf. Comp. Vision*, 1990, pp. 22–26.
- [5] J. Hadamard, "Sur les problemes aux drives partielles et leur signification physique," *Princeton University Bulletin*, pp. 49–52, 1902.
- [6] A. Bainbridge-Smith and R. Lane, "Measuring confidence in optical flow estimation," *IEEE Electronics Letters*, pp. 882–884, 1996.
- [7] M. Bertero, T. A. Poggio, and V. Torre, "Ill-posed problems in early vision," in *Proceedings of the IEEE*, 1988, pp. 869–889.
- [8] J. Barron, D. J. Fleet, and S. Beauchemin, "Performance of optical flow techniques," *Int. J. of Computer Vision*, vol. 12, no. 1, pp. 43–77, 1994.
- [9] E. P. Simoncelli, "Distributed representation and analysis of visual motion," Ph.D dissertation, p. 54, 1993.
- [10] M. J. Black and P. Anandan, "Robust dynamic motion estimation over time," in *Computer Vision and Pattern Recognition*, 1991, pp. 296–302.
- [11] H. Haussecker, H. Spies, and B. Jähne, "Tensor-based image sequence processing techniques for the study of dynamical processes," in *Int. Symp. Real-time Imaging and Dynamic Analysis*, 1998, pp. 704–711.
- [12] N. Ohta, "Movement vector detection with reliability indices," in *IAPR Workshop on Machine Vision Applications*, 1990, pp. 177–180.
- [13] A. Bruhn and J. Weickert, "A confidence measure for variational optic flow methods," pp. 283–298, 2006.
- [14] C. Kondermann, D. Kondermann, B. Jähne, and C. Garbe, "An adaptive confidence measure for optical flows based on linear subspace projections," in *DAGM*, 2007, pp. 132–141.
- [15] C. Kondermann, M. Rudolf, and C. Garbe, "A statistical confidence measure for optical flows," in *ECCV*, 2008, pp. 290–301.
- [16] G. H. Golub and C. F. V. Loan, *Matrix Computations*, 3rd ed. Johns Hopkins University Press, 1996.
- [17] T. Lindeberg, A. Akbarzadeh, and I. Laptev, "Galilean-diagonalized spatio-temporal interest operators," in *ICPR*, 2004, pp. 57–62.
- [18] H. Anton and C. Rorres, *Elementary Linear Algebra: Applications Version*, 7th ed. Wiley, 1994.
- [19] S. Baker, D. Scharstein, J. P. Lewis, S. Roth, M. Black, and S. R., "A database and evaluation methodology for optical flow," in *Int. Conf. Computer Vision*, 2007, pp. 1–8.
- [20] B. McCane, K. Novins, D. Crannitch, and B. Galvin, "On benchmarking optical flow," *Computer Vision and Image Understanding*, vol. 84, pp. 126–143, 2001.
- [21] [Online]. Available: <http://www.cs.brown.edu/~black/>

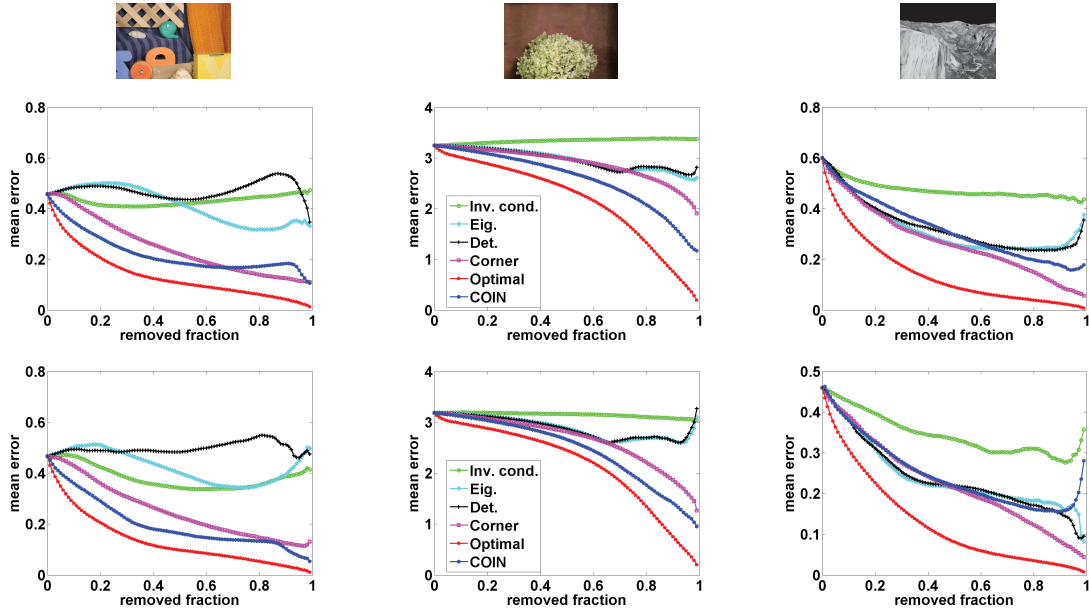


Fig. 1: Comparison of various measures on RubberWhale, Hydrangea and Yosemite (from left to right). In each column, and from top to bottom: the test image; the performance curves of different measures for flow computed on local  $7 \times 7$  patches; the performance curves of different measures for flow computed on local  $19 \times 19$  patches. The lower curve indicates better performance, where the lowest one corresponds to the theoretically ideal performance. All plots have the same legends.

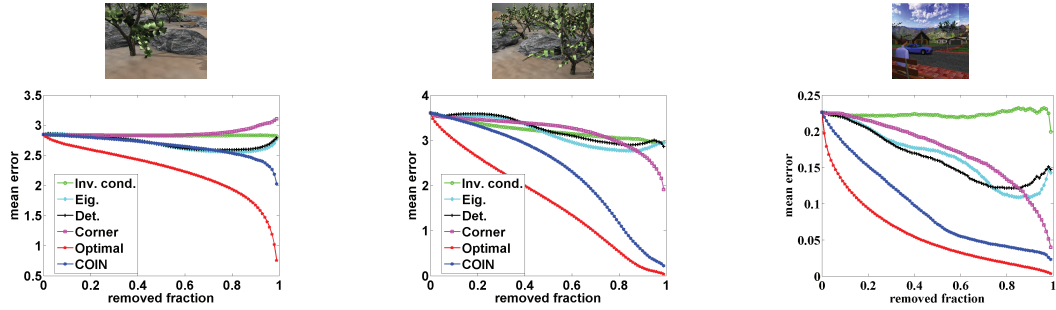


Fig. 2: Comparison of various confidence measures on Grove2, Grove3 and Street (from left to right). The lowest curve indicates the theoretically ideal performance. The COIN measure achieves best performance on all three sequences.

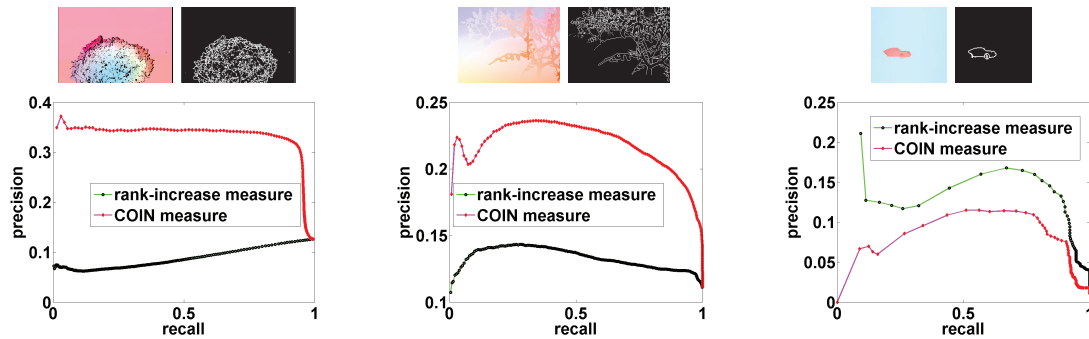


Fig. 3: Motion boundary detection results on RubberWhale, Grove3 and Street. The 1st row: the color-coded ground truth flows and the binary ground truth motion boundary maps. The second row: The recall-precision curves of motion boundary detection by the rank-increase measure and the COIN measure. The higher curve indicates better performance.